ELSEVIER

Melting Characteristics Along a Bundle of Horizontal Heated Cylinders Immersed in a Liquid Ice Layer

Masahiko Yamada
Shoichiro Fukusako
Hisashi Morizane
Department of Mechanical Engineering, Hokkaido University, Sapporo, Japan

Myoung-Hwan Kim
Department of Marine Engineering, Korea Maritime University, Pusan, Korea

Wilhelm Schneider
Institut für Strömungslehre und Wärmeübertragung, Technische Universität Wien, Wien, Austria

■ Experiments were performed to investigate the melting of liquid ice along a bundle of horizontal heated cylinders. A mixture of fine ice particles and ethylene glycol aqueous solution was adopted as the liquid ice for the test. In one set of experiments, the liquid ice was a quiescent layer, whereas in a second set of experiments the liquid ice was a fluidized bed layer. Measurements were carried out for a range of parameters such as initial concentration of aqueous binary solution, heat flux, and airflow rate for fluidization. The heat transfer coefficient for the fluidized liquid ice bed was found to be more than 25 times as large as that for the quiescent liquid ice bed.

Keywords: *melting heat transfer, thermal storage system, liquid ice, fluidized bed*

INTRODUCTION

Melting phenomena are encountered extensively in nature and in a variety of technologically important processes. The melting phenomenon is related to a wide variety of engineering fields: purification of metals, welding, electroslag melting, thawing of moist soil, and latent heat-of-fusion thermal energy storage are only a few of the important applications. Melting is a phase transformation process that is accompanied by absorption of thermal energy. The essential features of the system that exhibits melting phenomena are the existence of a liquid–solid interface that separates the two phases possessing different thermophysical properties and the absorption of thermal energy at the interface. The major problem in melting is thus to determine transport phenomena of the latent and sensible heat of the system. There is quite a large body of literature concerned with a variety of such problems in engineering as well as in the applied sciences. Recent reviews are available [1–4]. For conventional ice storage systems using common ice as a phase-change material (PCM), it has been demonstrated [9–13] that the melting heat transfer performance decreases with time because the heating tube and the ice tend not to be in contact with each other.

Recently, great attention has been paid to "liquid ice" as a new PCM instead of common ice alone, because liquid ice can be continuously produced and in practice can be transported by pipe. In addition, the cold/heat removal performance of liquid ice can be controlled. Therefore, the use of a thermal storage system using liquid ice [14] has been examined. However, there remain a variety of unknown characteristics with respect to releasing cold heat from liquid ice.

The objective of the present paper is to study the melting phenomena as well as the heat transfer characteristics along a bundle of horizontal heated cylinders immersed in liquid ice. In one set of experiments, the liquid ice was a quiescent layer, while in a second set of experiments the liquid ice was a fluidized bed layer. The effects of the initial concentration of aqueous binary solution, heat flux, and airflow rate for fluidization on melting heat transfer were extensively determined.

EXPERIMENTAL APPARATUS AND PROCEDURES

Experimental Apparatus

A schematic diagram of the experimental apparatus is depicted in Fig. 1. The essential components of the apparatus are the test section, an aqueous binary solution circulating loop, a cooling brine circulating loop, an air-supply loop, and the associated instrumentation.

Figure 2 shows the details of the test section, which consists of a test vessel, a distributor, and a calming section. The test vessel is made of a transparent acrylic box with inner dimensions of 270 × 240 × 90 mm, with the front and back made of double-pane glass to enable observation of the phenomena within the apparatus. A bundle of heated cylinders (11 cylinders 20 mm in diameter, three-step staggered array, and 50 mm in pitch) were installed horizontally within the test vessel, whose center is 100 mm from the distributor.

Address correspondence to Professor S. Fukusako, Department of Mechanical Engineering, Hokkaido University, N13-W8, Sapporo 060, Japan.

Experimental Thermal and Fluid Science 1996; 12:305–312

655 Avenue of the Americas, New York, NY 10010

0894-1777/96/$15.00
SSDI 0894-1777(95)00082-8

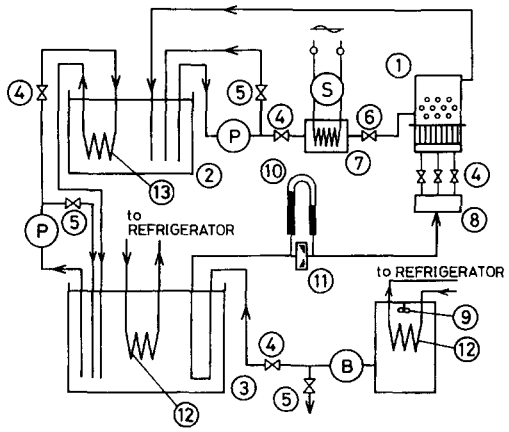

Figure 1. Schematic diagram of experimental apparatus. 1, test section; 2, ethylene glycol tank; 3, brine tank; 4, control valve; 5, bypass valve; 6, stop valve; 7, heater box; 8, distributor; 9, fan; 10, manometer; 11, orifice; 12, evaporator; 13, heat exchanger; P, pump; S, slidac; B, blower.

To measure the temperature within the vessel, six chromel-alumel thermocouple probes with a traversing device were inserted. The distributor consists of a piece of 200 mesh brass wire screen sandwiched between two perforated lucite plates with staggered holes 2.6 mm in diameter spaced 10 mm apart center to center. To ensure uniform airflow, a calming section of honeycomb design was set at the bottom of the test vessel.

Figure 3 indicates schematically the details of the heated cylinder. The cylinder was made of an acrylic pipe on which stainless steel foil 50 μm thick and 18 mm wide was spirally wound to ensure uniform heat flux conditions. To measure the surface temperature of the heated cylinder, 13 chromel-alumel thermocouples (0.1 mm O.D.) were attached to the back of the stainless steel foil through the mica foil (10 μm in thickness) at circumferential fixed intervals of 15°. In addition, the thermocouples were installed at three locations (center and ± 25 mm axial distance from the center) to confirm the axial uniformity of the temperature. The uncertainty of the temperature measurement, which includes both the precision of thermocouples and that of the micro voltage meter, is estimated to be $\pm 0.8\%$. The cylinder surface was coated with teflon for insulation as shown in Fig. 3. The temperature difference between the surface of the cylinder and the thermocouples is so small that it can be neglected. To avoid heat input from the end of the heated cylinder, thermal insulation was put into the cylinder.

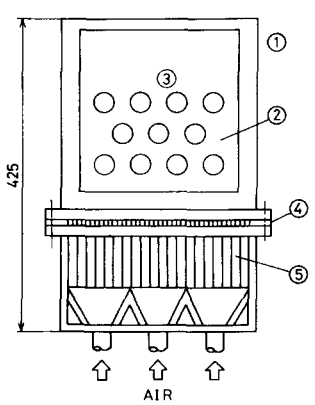

Figure 2. Details of test section. 1, Test section; 2, double-pane glass; 3, heating tube bundle; 4, distributor; 5, honeycomb.

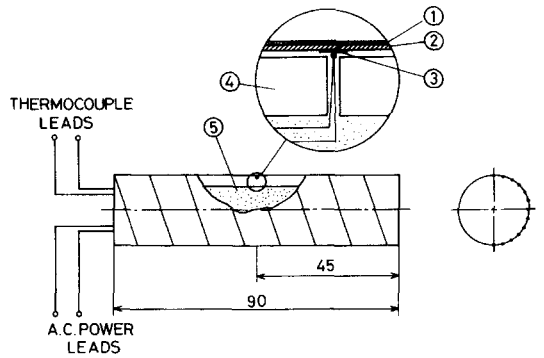

Figure 3. Details of heated cylinder. 1, PTFE coating; 2, stainless steel sheet; 3, mica sheet; 4, Lucite tube; 5, insulation. (●) Thermocouple.

Air was used to make a fluidized liquid ice bed. Dry air was prepared in a temperature-regulated (about -20°C) chamber whose flow rate was measured by use of an orifice. Using an electric heater, the temperature of the supplied air was controlled so as to be equal to the bulk temperature of the fluidized liquid ice bed.

Experimental Procedures

The liquid ice used in the experiment was a mixture of fine ice particles (average 500 μm in diameter), which were made in a temperature-regulated room (about -25°C) over a period of more than 6 months, and ethylene glycol aqueous solution.

The ice particles and the aqueous binary solution, which were each maintained at the equilibrium freezing temperature corresponding to the concentration of the aqueous binary solution, were mixed in the desired proportion just before the experiment. An ice packing factor (IPF) of 62% was adopted throughout the experiments. Three ethylene glycol aqueous solutions with initial concentrations of 10, 20, and 30 wt % were used as the test liquids. The start of the experiment was defined as the time at which the electric input to the heated cylinders was initiated.

Photographs of the melting phenomena were taken at appropriate intervals. The temperature of the heated cylinder surface and that of the testing vessel were continuously recorded. To avoid heat input from the environment, the test section was carefully covered with insulation (styrofoam of 100 mm thickness) except during observation.

To counter the effect of air enthalpy on the heat balance, the temperature of the air supply was controlled so as to be equal to the bulk temperature of the fluidized liquid ice bed by using an electric heater installed in the mixing box.

The local heat transfer coefficient h_θ and average heat transfer coefficient h were respectively evaluated according to the following equations with 1.8% precision, which includes uncertainties of both temperature and heat flux.

$$h_\theta = \frac{Q_{\text{input}} - Q_{\text{loss}}}{A(T_{w\theta} - T_b)} \quad (1)$$

and

$$h = \frac{1}{\pi}\int_0^\pi h_\theta \, d\theta. \quad (2)$$

It was found that heat loss from the end of the heated cylinder, Q_{loss}, was generally less than 0.5% of the total heat input from the heated cylinder. The heat loss Q_{loss} was evaluated as the temperature difference between the thermocouples embedded in the Bakelite cylinder that was connected to the test cylinder. Then Q_{loss} was neglected for the practical calculations in Eqs. (1) and (2).

The mean value of the temperatures at the six locations in the test vessel was taken as the bulk temperature T_b. Thermophysical properties of both ethylene glycol aqueous solution and ice were based on the data of [14, 15].

RESULTS AND DISCUSSION

Melting Characteristics of Solid–Liquid Two-Phase Quiescent Liquid Ice Bed

Figure 4 shows the melting behavior along a bundle of horizontal heated cylinders immersed in a quiescent liquid ice bed versus time. The results were obtained under the conditions of $D = 0.02$ m, $C_{0i} = 30$ wt %, and $q = 1.5 \times 10^3$ W/m^2, which are represented in Figs. 4*a–d* at $t = 30$, 40, 50, and 60 min, respectively. As shown in Fig. 4*a*, the melting interface tends to advance remarkably in the horizontal direction [12], which is quite different from the common melting behavior observed when common ice [9, 16] or PCM [17, 18] around a horizontal heated cylinder melts; namely, the melting interface proceeds mainly in the vertical direction to become "pear shaped." This is attributed to the fact [12] that stratified layers that occur in a melt region owing to double diffusion of coupled heat and mass transfer prevent the upward movement of the melt in the vertical direction. As time elapses, the melt regions tend to combine with others both horizontally and vertically and to eventually merge into a single melt region in which a bundle of cylinders are immersed (see Fig. 4*d*).

Heat Transfer Characteristics of Solid–Liquid Two-Phase Quiescent Liquid Ice Bed

Figure 5 shows the distributions of the local heat transfer coefficient along the heated cylinder (central one of a bundle of cylinders), using time as a parameter. The abscissa denotes the angle θ (in degrees) from the bottom of the heated cylinder. The characteristics at $t = 30$ min are similar to those for a single cylinder [12]; the melting interface tends to advance remarkably in the horizontal direction. For time t from 30 to 40 min, the heat transfer

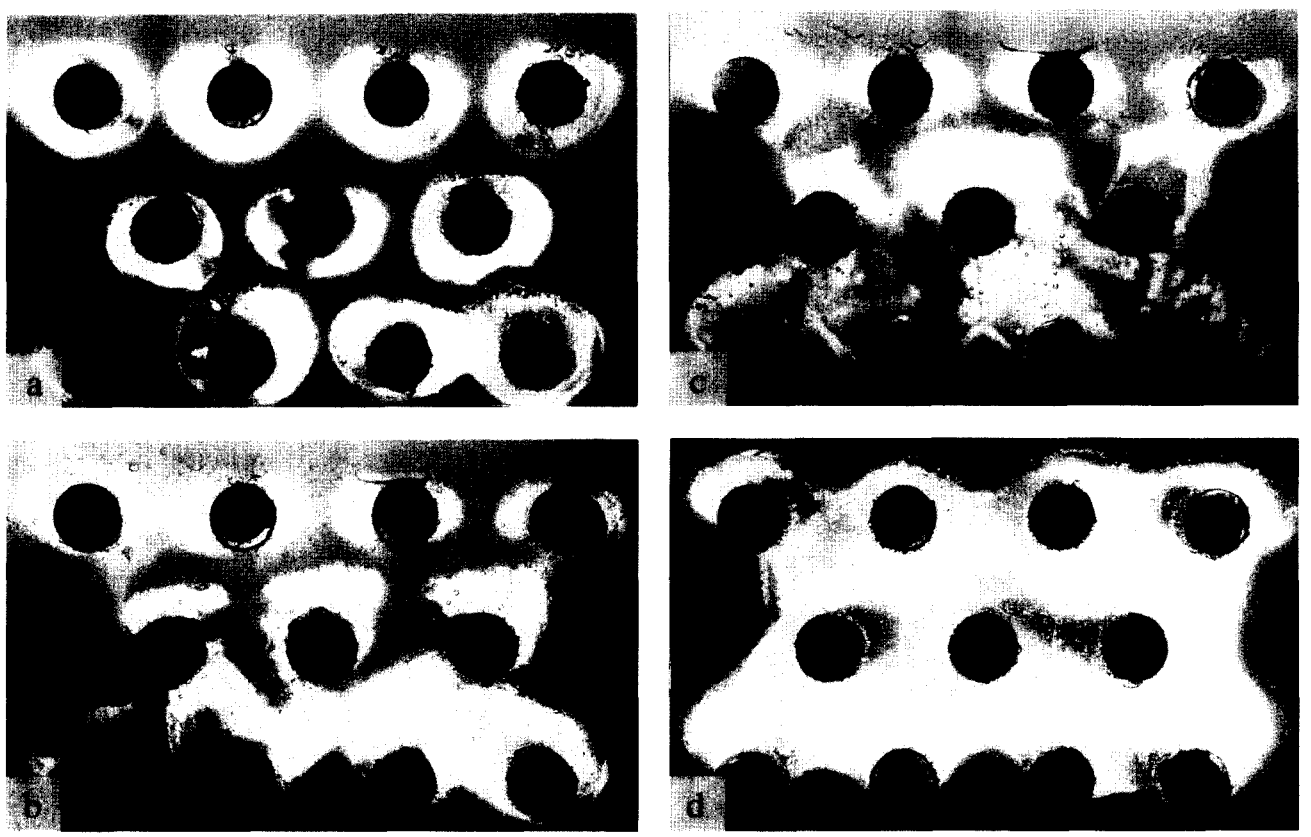

Figure 4. Melting behavior of solid–liquid two-phase quiescent liquid ice bed.

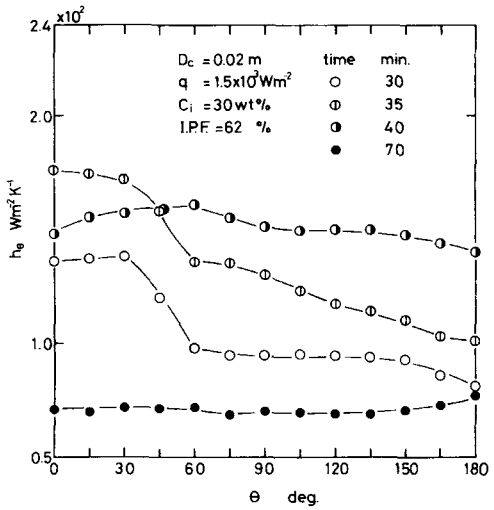

Figure 5. Local heat transfer coefficient behavior.

increases markedly (in particular, in the upper portion of the heated cylinder, $\theta > 60°$), then decreases abruptly, which is different behavior from that of a single cylinder [12]. This may be due to the combining of the melting regions shown in Figs. 4*b* and *c*.

There are stratified layers in the melt region along a heated cylinder [12], in which both the temperature and concentration of the lower melt region are in general greater than those of the upper melt region; the existence of the stratified layers obstructs smooth convection in the melt region. Therefore, the connection of the upper and lower melt regions (see Fig. 4*b*) causes a mixing of the liquids; consequently, the liquid of low temperature and low density around the lower cylinder rises into the melt liquid below the upper cylinder, which destroys the stratified layers and motivates convection, thus resulting in an increase in the heat transfer coefficient (see the data for t = 35 and 40 min in Fig. 5).

Figure 6 represents the characteristics of average heat transfer coefficient versus time. The data for C_{0i} = 30 wt % in the figure correspond to those in Fig. 5. The general trend through the data is that the average heat transfer coefficient first decreases sharply with time, takes a minimum, increases to obtain a maximum, then decreases gradually to approach an approximately constant value. The sharp decrease in heat transfer at the beginning stage of the experiment is considered to confirm that the heat transfer is controlled mainly by conduction; a sharp increase in heat transfer after taking a minimum results from the combination of the melt regions along both the upper and lower cylinders.

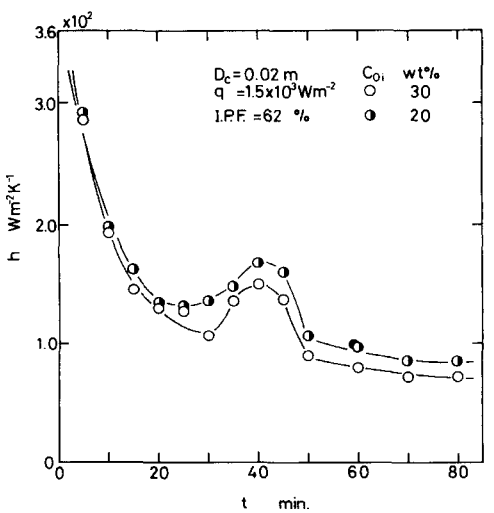

Figure 6. Average heat transfer coefficient behavior.

Characteristics of a Solid–Air–Liquid Three-Phase Fluidized Liquid Ice Bed

Figure 7 shows the representative fluidization behavior of the solid–air–liquid three-phase fluidized liquid ice bed. As shown in Fig. 7, air bubbles hitting the lowest-row, second-row, and third-row cylinders are divided into smaller ones row after row, which confirms that agitation of a three-phase fluidized bed for a bundle of cylinders is improved favorably compared with that for a single cylinder [12]. Thus for a bundle of heated cylinders immersed in a three-phase fluidized liquid ice bed, contact between ice particles, which are accompanied by air bubbles, and heated cylinders may be markedly promoted.

Average Heat Transfer Coefficient Characteristics

Representative Characteristics of Heat Transfer Figures 8 and 9 show the horizontal and vertical distributions of the average heat transfer coefficient within a three-row bundle of cylinders (total of 11 cylinders) immersed in the fluidized liquid ice bed. The figures reveal that the average heat transfer coefficient for any cylinder within a cylinder bundle is uniform both horizontally and vertically, thus yielding quite favorable fluidization characteristics of the current system. Therefore, the following discussion on heat transfer characteristics is for a central cylinder within a cylinder bundle.

Figure 10 plots the representative characteristics of both the average heat transfer coefficient along a bundle of heated cylinders immersed within the fluidized liquid ice bed and the bulk temperature of the bed versus time.

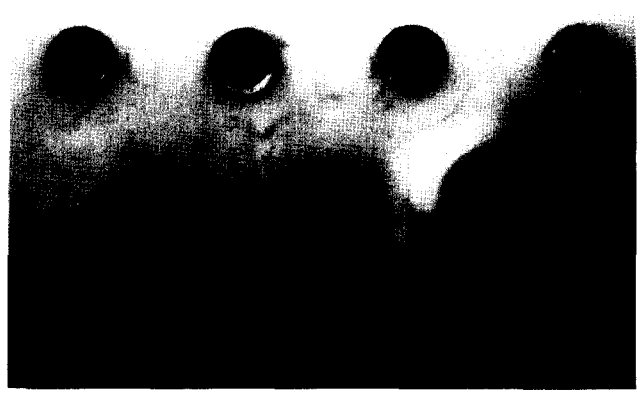

Figure 7. Fluidization of solid–air–liquid three-phase liquid ice bed.

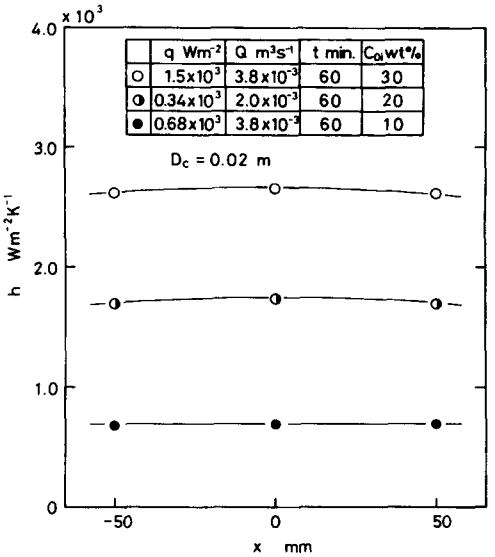

Figure 8. Horizontal distribution of heat transfer coefficient.

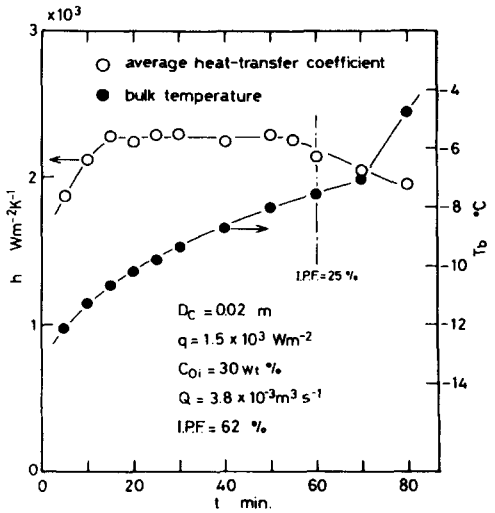

Figure 10. Characteristics of average heat transfer coefficient and bulk temperature.

It is seen in the figure that the average heat transfer coefficient may be uniform except during the early stages of the experimental run. However, the heat transfer coefficient tends to decrease when the IPF becomes smaller than about 25% owing to melting of the ice particles.

On the other hand, the bulk temperature in the fluidized bed (corresponding to the equilibrium freezing temperature of the aqueous binary solution) is found to increase monotonically with melting of the ice particles. When a cylinder is heated under the condition of uniform heat flux, the surface temperature of the heated cylinder increases monotonically over time, thus resulting in the heat transfer characteristics shown in Fig. 10, which were commonly observed (see Figs. 10–13) throughout the experimental run.

Effect of Airflow Rate Figure 11 shows the effect of airflow rate on the average heat transfer coefficient. The three groups of data correspond to airflow rates of $Q = 1.0 \times 10^{-3}$, 2.0×10^{-3}, and 3.8×10^{-3} m^3/s. As seen in the figure, the heat transfer increases with an increase in airflow rate. For the common solid–gas two-phase fluidized bed, heat transfer tends to decrease for superficial air velocity (airflow rate) above a certain value, because the porosity of the bed increases to decrease the particle density along the heated cylinder [19, 20].

On the other hand, for the current solid–air–liquid three-phase fluidized liquid ice bed, the ice particles may float within the liquid owing to their buoyancy or may cling to the air bubble surface. Then the decrease in particle density in the current system appears to be small compared with that of the solid–air two-phase fluidized bed, thus leading to the maintenance of an efficient fluidized bed.

Effect of Heat Flux The effect of heat flux on the average heat transfer coefficient is demonstrated in Fig. 12. As expected, increasing the heat flux causes an increase in the average heat transfer coefficient. It is seen in the figure that for $q = 1.5 \times 10^3$ W/m^2, the average heat transfer coefficient decreases sharply after $t = 60$ min. This may be due to a decrease in IPF to less than about 25% (see Fig. 10) owing to melting of the ice particles.

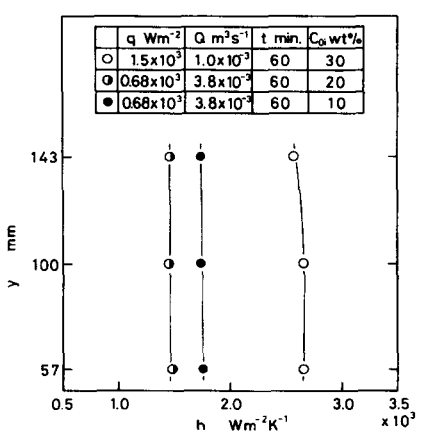

Figure 9. Vertical distribution of heat transfer coefficient.

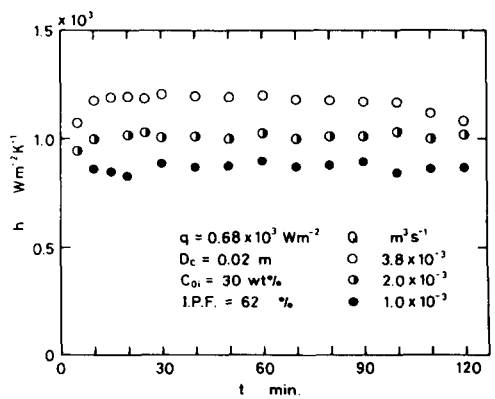

Figure 11. Effect of airflow rate on average heat transfer coefficient.

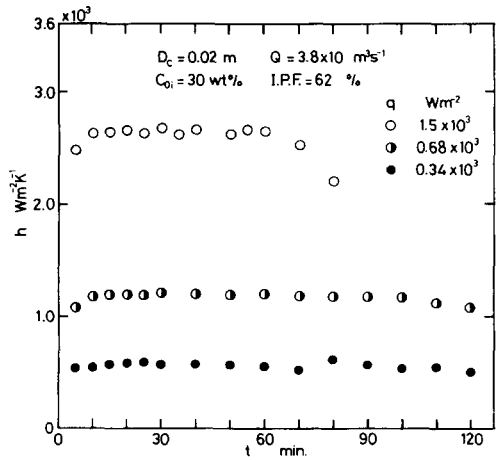

Figure 12. Effect of heat flux on average heat transfer coefficient.

Effect of Initial Concentration of Aqueous Binary Solution
Figure 13 indicates the effect of initial concentration of aqueous binary solution on the average heat transfer coefficient. From this figure it is seen that decreasing the initial concentration of the aqueous binary solution leads to an increase in heat transfer. This may be attributed mainly to the difference in thermophysical properties; the heat capacity of the liquid ice increases whereas the viscosity of the ethylene glycol aqueous solution decreases when the concentration of the solution decreases (this corresponds to a higher bed temperature).

Heat Transfer and Its Control Characteristics in a Solid–Air–Liquid Three-Phase Fluidized Liquid Ice Bed

Figure 14 shows the heat transfer performance of the solid–air–liquid three-phase liquid ice fluidized bed. In this figure, the ordinate variable is the ratio of the average heat transfer coefficient for the solid–air–liquid three-phase liquid ice bed (e.g., arithmetic mean value of the average heat transfer coefficient for t = 15–55 min in Fig. 10), h_m, to that for the solid–liquid two-phase quiescent bed [12], h_{fb}. The abscissa variable is the heat flux, and the parameter is the airflow rate.

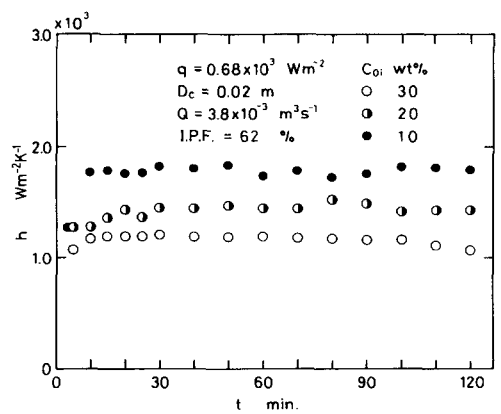

Figure 13. Effect of initial concentration on average heat transfer coefficient.

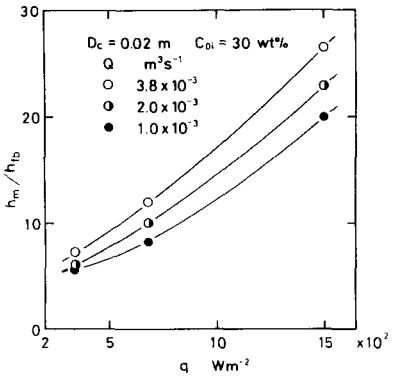

Figure 14. Heat transfer performance of solid–air–liquid three-phase fluidized bed.

It is seen from Fig. 14 that the heat transfer coefficient for the three-phase liquid ice bed may be about 6–27 times as large as that for the two-phase quiescent liquid ice bed. Furthermore, the figure indicates that for any heat flux the airflow rate may be a useful factor in the control of heat transfer.

Characteristics of Dynamic Force for Fluidization

It is well known that pressure loss through a fluidized bed is constant irrespective of the airflow rate after fluidization of the particle bed occurs. The dynamic power for fluidization of the particle bed is, in general, given as

$$N = U_0 \Delta p S. \tag{3}$$

Figure 15 represents the characteristics of the dynamic power for fluidization of the liquid ice bed. The ordinate variable is the ratio of the dynamic power for fluidization to the total heat transferred in a bundle of heated cylinders immersed within a fluidized liquid ice bed, while the abscissa variable is airflow rate. There are three groups of data corresponding to heat fluxes of 0.34×10^3, 0.68×10^3, and 1.50×10^3 W/m^2. As shown in the figure, the dynamic power ratio for fluidization, N/Q_{totl}, decreases as the heat flux increases. The figure also indicates that for $q = 1.5 \times 10^3$ W/m^2 the average heat transfer coef-

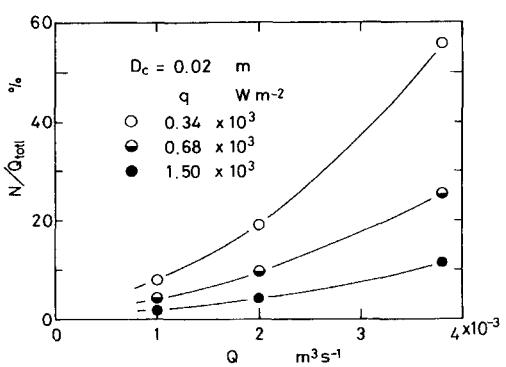

Figure 15. Power characteristics for fluidization of liquid ice bed.

ficient, which is about 20–27 times as large as that for the two-phase quiescent liquid ice bed, may be obtained by use of the dynamic power corresponding to about 10% of N/Q_{totl} (see Fig. 14).

PRACTICAL SIGNIFICANCE

One way of addressing load management for air conditioning is through the use of ice thermal storage. Great attention has been paid to "liquid ice," a mixture of ice particles in a liquid matrix, as a new PCM in place of ice alone, because liquid ice can be transported by pipe. In addition, quite efficient and controllable heat exchange can be expected.

The present extensive data on the characteristics of cold-heat exchange between a solid–liquid two-phase quiescent liquid ice bed or solid–air–liquid three-phase fluidized liquid ice bed and a bundle of heated cylinders for a variety of parameters provide a basis for other researchers to develop additional insight into the heat transfer mechanism of much more efficient cold-heat exchange.

Figures 11–15 should be quite useful for designers, public utility regulators, operators, and others in the air-conditioning community for developing more favorable cold-heat exchange equipment.

CONCLUSIONS

Experiments were carried out to determine the melting characteristics along a bundle of horizontal heated cylinders immersed within a liquid ice bed. Both the solid–liquid two-phase quiescent liquid ice bed and solid–air–liquid three-phase fluidized liquid ice bed were adopted. The following conclusions may be drawn within the parameters covered.

1. For the solid–liquid two-phase quiescent liquid ice bed, the melting interface between each two cylinders advances markedly in the horizontal direction owing to the stratified layers in the melt region. As time elapses, the melt regions along the respective cylinders tend to be coupled, which remarkably influences the melting heat transfer.
2. The heat transfer coefficient for the solid–air–liquid three-phase fluidized liquid ice bed increases with increasing heat flux and airflow rate as well as with decreasing initial concentration of the aqueous binary solution.
3. The heat transfer coefficient for the solid–air–liquid three-phase fluidized liquid ice bed may be about 27 times as large as that for the solid–liquid two-phase quiescent liquid ice bed, where the dynamic power for fluidization, which corresponds to about 10% of the total thermal energy transferred within a bundle of cylinders, is required.
4. The operation of heat exchange within a bundle of horizontal cylinders by use of a solid–air–liquid three-phase fluidized liquid ice bed can be quite useful from the viewpoint of heat transfer promotion as well as heat transfer control.

NOMENCLATURE

A	heat transfer area of heated cylinder, m^2
C_{0i}	initial concentration of aqueous binary solution, wt %
D	diameter of heated cylinder, m
h	average heat transfer coefficient, $W/(m^2\ K)$
h_{fb}	arithmetic mean value of average heat transfer coefficient in free-convection region for quiescent solid–liquid two-phase liquid ice bed, $W/(m^2\ K)$
h_m	arithmetic mean value of average heat transfer coefficient for solid–gas–liquid three-phase fluidized liquid ice bed, $W/(m^2\ K)$
h_θ	local heat transfer coefficient, $W/(m^2\ K)$
IPF	ice packing factor (mass ratio of ice to ethylene glycol aqueous solution), %
Δp	pressure loss, Pa
q	heat flux of heated cylinder, W/m^2
Q	airflow rate, m^3/s
Q_{input}	electricity input to heated cylinder, W
Q_{loss}	heat loss from end of heated cylinder, W
Q_{totl}	total heat transferred in a bundle of heated cylinders, W
S	sectional area of test vessel, m^2
T_b	bulk temperature of fluidized liquid ice bed, °C
$T_{w\theta}$	local surface temperature of heated cylinder, °C
t	elapsed time from start of experimental run, min
U_0	superficial air velocity, m/s
wt	mass fraction ratio, %
x	distance from center axis of test vessel, m
y	distance from distributor, m

Greek Symbols

θ	angle from bottom of heated cylinder, deg
λ	thermal conductivity, W/(m K)
ρ	density, kg/m^3

REFERENCES

1. Viskanta, R., Heat Transfer During Melting and Solidification of Metals, *J. Heat Transfer* **110,** 1205–1219, 1988.
2. Yao, L. S., and Prusa, J., Melting and Freezing, *Adv. Heat Transfer* **19,** 1–95, 1989.
3. Fukusako, S., and Yamada, M., Recent Advances in Research on Water-Freezing and Ice-Melting Problems, *Exp. Thermal Fluid Sci.* **6,** 90–105, 1993.
4. Fukusako, S., and Yamada, M., Recent Advances in Research on Melting Heat Transfer Problems, *Proc. 10th Int. Heat Transfer Conf.* **1,** 313–331, 1994.
5. Miyasaka, A., Current Trends of Ice Storage System in USA, *Refrigeration* **62,** 382–392, 1987.
6. Sagara, N., Performance of Glycol Ice Storage System with Ice-on-Coil Type Heat Exchanger, *Refrigeration* **62,** 393–401, 1987.
7. Yanagihara, Y., An Economic Study of Ice Storage Type HVAC Systems, *Refrigeration* **62,** 487–497, 1987.
8. Rieger, H., and Beer, H., The Melting Process of Ice Inside a Horizontal Cylinder: Effects of Density Anomaly, *J. Heat Transfer* **108,** 166–173, 1986.
9. Torikoshi, K., Yamashita, H., and Nakazawa, Y., An Experimental Study of Melting of Ice About Horizontal Cylinders, *Proc. ASME/JSME Thermal Eng. Conf.* **1,** 269–274, 1991.

10. Hirata, T., Makino, Y., and Kaneko, Y., Analysis of Natural Convection Inside Isothermally Heated Horizontal Rectangular Capsule, *Wärme Stofübertrag* **28,** 1–9, 1993.
11. Endo, M., and Hoshino, M., Crystallized Liquid Ice Thermal Storage System, *Refrigeration* **62,** 481–487, 1987.
12. Yamada, M., Fukusako, S., Morizane, H., and Kim, M. H., Melting Heat Transfer Along a Horizontal Tube Immersed in Liquid Ice, *JSME Int. J.* **36,** 345–350, 1993.
13. Fukusako, S., Yamada, M., Morizane, H., and Kim, M. H., Melting Heat Transfer Along a Horizontal Heated Tube Immersed in a Fluidized Liquid Ice Bed, *Exp. Thermal Fluid Sci.* **6,** 353–359, 1993.
14. *JSME Data Book: Thermophysical Properties of Fluids*, p. 353, 1986.
15. Fukusako, S., Thermophysical Properties of Ice, Snow, and Sea Ice, *Int. J. Thermophys.* **11,** 353–372, 1990.
16. Torikoshi, K., Nakazawa, Y., Kawabata, K., Yamamoto, H., and Fushimi, K., An Experimental Study of Melting of Ice About Horizontal Cylinders, 2nd Int. Symp. Cold Regulated Heat Transfer, pp. 45–50, 1989.
17. Abdel-Wahed, R. M., Ramsey, J. M., and Sparrow, E. M., Photographic Study of Melting About an Embedded Horizontal Heat Cylinder, *Int. J. Heat Mass Transfer*, **22,** 171–173, 1979.
18. Bathelt, A. G., and Viskanta, R., Heat Transfer at Solid–Liquid Interface During Melting from a Horizontal Cylinder, *Int. J. Heat Mass Transfer*, 1493–1503, 1980.
19. Fukusako, S., Seki, N., Ishiguro, S., and Eguchi, T., Heat Transfer from Horizontal Immersed Tube in Particles Bed, *Trans. JSME, Ser. B* **51**(463), 989–994, 1985.
20. Aihara, T., Maruyama, S., Aya, S., and Hongoh, M., Heat Transfer Characteristics of a Low-Pressure-Loss Fluidized-Bed Heat Exchanger with Single Row Tubes, *Trans. JSME, Ser. B* **52**(476), 1718–1725, 1986.

Received May 9, 1995; revised July 31, 1995